Rapid Communications

Deexcitation γ-ray transitions from the long-lived $I^{\pi} = 13/2^{+}$ metastable state in ^{195}Os

Y. X. Watanabe,[1,*] M. Ahmed,[2,1] Y. Hirayama,[1] M. Mukai,[2,1,3] J. H. Park,[4] P. Schury,[1] Y. Kakiguchi,[1] S. Kimura,[3] A. Ozawa,[2] M. Oyaizu,[1] M. Wada,[1,3] and H. Miyatake[1]

[1]*Wako Nuclear Science Center, Institute of Particle and Nuclear Studies, High Energy Accelerator Research Organization (KEK), Tsukuba, Japan*

[2]*Tsukuba University, Tsukuba, Japan*

[3]*Nishina Center for Accelerator-Based Science, RIKEN, Wako, Japan*

[4]*Institute for Basic Science, Daejeon, Korea*

(Received 12 November 2019; accepted 20 March 2020; published 21 April 2020)

Deexcitation γ rays associated with an isomeric state of the ^{195}Os were measured for the first time. The half-life of the isomeric state of the neutral atom ^{195m}Os was deduced. The isomers were produced in multinucleon transfer reactions between ^{136}Xe beams and ^{198}Pt targets, and were collected and separated by KEK Isotope Separation System. Analysis of γ-γ correlation and comparison with previous measurement of the isomeric state using the ESR at GSI Darmstadt suggests a possible decay scheme of ^{195m}Os.

DOI: 10.1103/PhysRevC.101.041305

The neutron-rich nuclei of W, Os, and Pt with the mass number of 180–200 are predicted to exhibit characteristic structural evolution due to a complex interplay between the single-particle and collective degrees of freedom [1–5]. The shape is changed from prolate to oblate as their mass numbers increase. In the case of osmium isotopes ($Z = 76$), the ^{194}Os is suggested to be prolate deformed experimentally [6]. However, a more recent experimental study revealed its γ softness, indicating it is in the transitional region [7]. Spectroscopic information of such shape transitional nuclei is considered to provide crucial inputs to their theoretical predictions. Steer *et al.* [8] observed γ cascade transitions from a short-lived isomer of the ^{195}Os which were assumed to feed a neutron $13/2^{+}[606]$ state. It is expected as a long-lived isomer located at the low-energy above the neutron $3/2^{-}[501]$ ground state of the ^{195}Os. Reed *et al.* [9] identified an isomeric state at the excitation energy of 454(10) keV for the ^{195}Os^{76+} using the ESR at GSI Darmstadt. The half-life of such isomeric state, ^{195m}Os^{76+}, was evaluated to be >9 min. Here, we present the results of half-life measurement for the isomeric state of the neutral atom, ^{195m}Os.

Multinucleon transfer reactions between ^{136}Xe and ^{198}Pt have an advantage to access neutron-rich nuclei with neutron numbers around 126 [10]. The same γ transitions from the short-lived isomer of ^{195}Os in Ref. [8] were observed in ^{195}Os isotopes produced by the multinucleon transfer reaction, indicating their population of the short-lived isomer leading to the long-lived isomer ^{195m}Os [11,12]. ^{136}Xe beams provided by the RRC accelerator at RIKEN RIBF facility, which impinged on rotating ^{198}Pt targets of thickness 12.5 mg/cm^2, were used to populate the ^{195m}Os. The beam energy was degraded by a rotating stack of three titanium foils of thickness 3 μm each from energy 10.75 MeV/nucleon to 9.4 MeV/nucleon to maximize the yields of reaction products ejected from the targets. The typical beam intensity was 50 pnA on the targets. The nuclei of interest were collected and separated by KEK Isotope Separation System (KISS) [13], which is an isotope separator on-line with a gas-cell-based laser ion source. Reaction products ejected from the targets passed through a polyimide film of thickness 5 μm into a doughnut-shaped gas cell [14], which was filled with highly pure argon gas of pressure 88 kPa. They were thermalized and neutralized in the argon gas, and those neutral atoms were transported to the exit of the gas cell. They were irradiated with two-color lasers for element-selective ionization with the laser resonance ionization technique just before the exit of the gas cell. The ionization scheme of osmium was investigated before the experiment [15]. A laser of wavelength 247.7590 nm from a frequency-tunable dye laser pumped by a XeCl:excimer laser was used for the excitation of the ^{195m}Os atomic level with the other laser of wavelength 307.9 nm from another XeCl:excimer laser for the ionization. The ions ejected from the gas cell were transported by a stack of three multipole RF ion guides, and were accelerated by a high voltage of 20 kV. They were mass-separated by a dipole electromagnet, and were implanted into an aluminized Mylar tape of thickness 12.5 μm.

The multisegmented proportional gas counter (MSPGC) [16] was placed surrounding the tape to detect β rays, x rays, and conversion electrons in the decay of the implanted radioactive nuclei. The MSPGC consists of two concentric layers of 16 proportional gas counter tubes each. The geometry is 200 mm in height and 90 mm in outer diameter. A hit pattern analysis of those 32 gas counter tubes makes it possible to separate different kinds of events. The hit pattern "$M = 1$", where only one counter tube in the inner layer fires, is sensitive to x rays and low-energy conversion electrons

*yutaka.watanabe@kek.jp

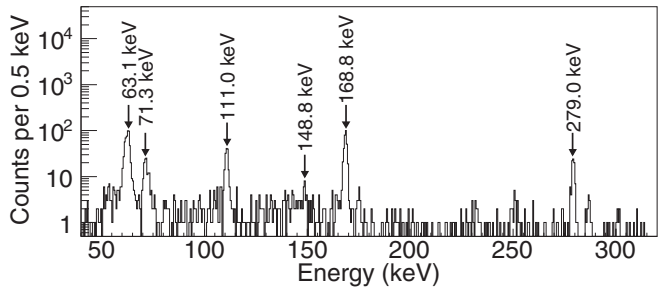

FIG. 1. γ-ray energy spectrum in coincidence with the MSPGC hit pattern "$M = 1$".

by suppressing the events owing to the energetic β rays. Four high-purity germanium (HPGe) clover detectors were placed surrounding the MSPGC to detect γ rays. With the compact configuration of the experimental setup, where the distances between the surfaces of the HPGe clover detectors and the tape were around 5 cm, the total absolute detection efficiency for full-energy peaks was about 16% for 150-keV γ rays. The beams from KISS were pulsed by an electrostatic deflector before the dipole electromagnet with time cycles of 120-s beam-on and 240-s beam-off periods. The tape

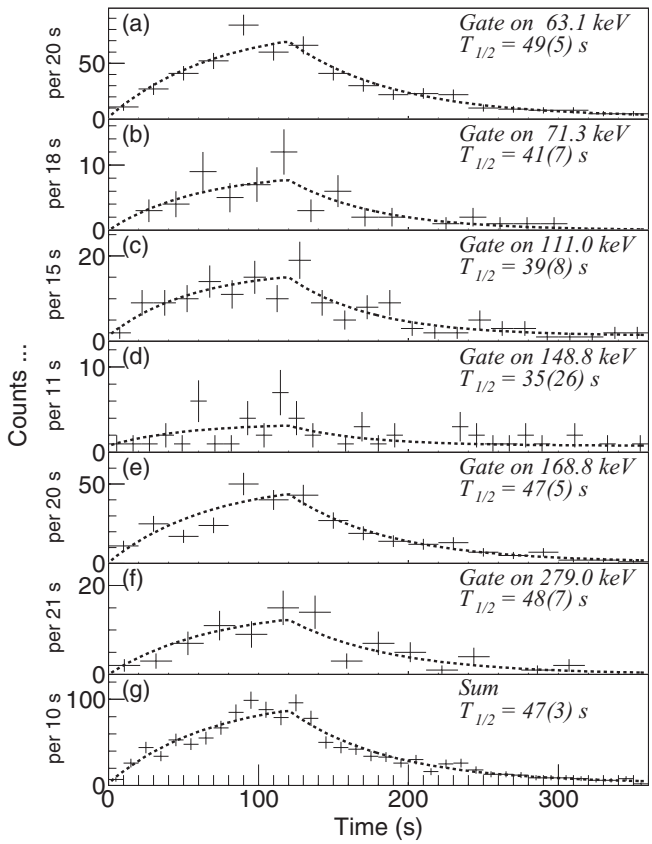

FIG. 2. Time distributions of detected counts for x rays and γ rays corresponding to six peaks in Fig. 1 [(a) 63.1 keV, (b) 71.3 keV, (c) 111.0 keV, (d) 148.8 keV, (e) 168.8 keV, and (f) 279.0 keV]. (g) shows sum of them. Number in parenthesis of each figure indicates statistical error.

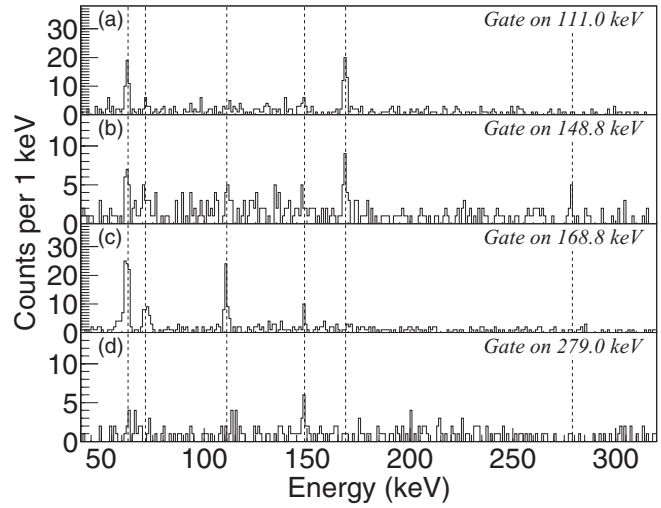

FIG. 3. γ-ray energy spectra in coincidence with other γ rays of indicated energies.

was moved vertically by about 30 cm after each cycle to eliminate radioactivities from the preceding implantation and the accumulated daughter nuclei.

Figure 1 shows γ-ray energy spectrum in coincidence with the MSPGC hit pattern "$M = 1$". Four peaks were found at 111.0(1), 148.8(2), 168.8(2), and 279.0(2) keV with two peaks at 63.1(1) and 71.3(1) keV, which correspond to $K_{\alpha 1}$ and $K_{\beta 1}$ x rays of the osmium, respectively. The observation of those characteristic x rays of the osmium suggests that the detected γ rays of four peaks in the spectrum are due to isomeric decays of the ^{195}Os.

Figures 2(a)–(f) show detected counts of those x rays and γ rays as functions of time. Those were obtained by gating six

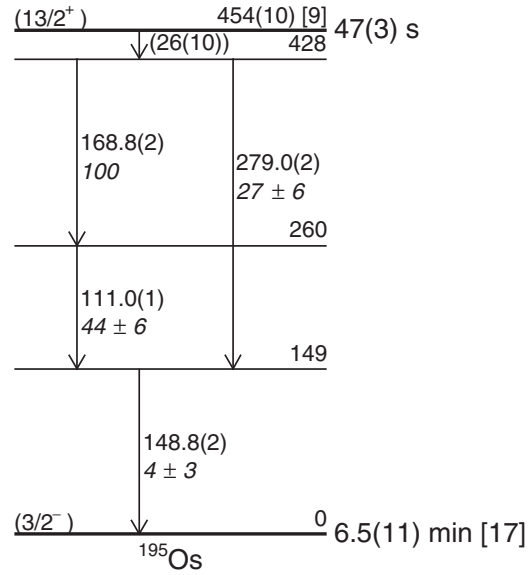

FIG. 4. Possible decay scheme of isomeric state of ^{195}Os. Labels with arrows indicate the γ-ray energies in keV. Relative γ-ray intensities are also shown in italics. See the text for details.

TABLE I. Evaluated ranges of conversion coefficients, α, partial half-lives of γ transition, $T^{\gamma}_{1/2}$, and Weisskopf estimation for half-lives of electric and magnetic transitions, $T^{\mathrm{W}}_{1/2}$, for the 26-keV transition with possible multipolarities including uncertainty of 10 keV.

Multopolarity	α	$T^{\gamma}_{1/2}$	$T^{\mathrm{W}}_{1/2}$	$T^{\mathrm{W}}_{1/2}/T^{\gamma}_{1/2}$
$E1$	1.2×10^{0}-1.1×10^{1}	1.7 min–9.4 min	4.3 ps–49 ps	10^{-14}-10^{-13}
$M1$	2.0×10^{1}-2.2×10^{2}	16 min–2.8 h	0.47 ns–5.4 ns	10^{-13}-10^{-12}
$E2$	4.9×10^{2}-2.8×10^{4}	6.4 h–15 d	0.14 ms–8.0 ms	10^{-9}-10^{-8}
$M2$	1.4×10^{3}-6.4×10^{4}	18 h–35 d	15 ms–0.88 s	10^{-7}-10^{-6}
$E3$	3.8×10^{4}-4.9×10^{6}	21 d–7.3 yr	1.9 h–23 d	10^{-3}-10^{-2}
$M3$	1.1×10^{5}-2.2×10^{7}	60 d–33 yr	8.7 d–7.0 yr	10^{-1}-10^{0}
$E4$	1.5×10^{6}-4.2×10^{8}	2.2 yr-6.3×10^{2} yr	1.6×10^{4} yr-2.3×10^{7} yr	10^{4}-10^{5}
$M4$	5.7×10^{6}-2.8×10^{9}	8.5 yr-4.2×10^{3} yr	1.7×10^{6} yr-2.6×10^{9} yr	10^{5}-10^{6}

peaks on the spectrum in Fig. 1. The half-life characteristic to each gated time spectrum was deduced with a function of a growth curve, a decay curve, and a constant background, which is shown by a dotted line in each panel of Fig. 2. The obtained half-lives are indicated in panels of Fig. 2, and they agree with each other within their errors. The panel (g) indicates the sum of all gated time spectra and the result. The obtained half-life is 47(3) s, which is shorter than the half-life of the ground state of the ^{195}Os, 6.5(11) min [17]. Therefore those newly found four γ transitions are considered to be associated with decay of one isomeric state in the ^{195}Os with the half-life of 47(3) s.

To get inspection of the decay scheme of those four γ transitions, γ-γ coincidence analysis was performed. Figure 3 shows γ-ray energy spectra with gates of those four γ rays, as indicated in panels. Vertical dashed lines on the spectra indicate energies of x rays and γ rays of interest. First of all, two characteristic x rays associated to osmium atoms can be seen in all of gated spectra, which is another evidence that these four γ transitions belong to the isomeric state in osmium.

Gating 148.8-keV γ rays, the spectrum (b) shows peaks of all other three γ-ray energies. However, gating 279.0-keV γ rays, the peak at 148.8 keV was only found in the spectrum (d). The spectra (a) and (c) with gates on 111.0- and 168.8-keV γ rays, respectively, also do not show any peaks at 279.0 keV. They suggest that the 111.0- and 168.8-keV transitions occur in series, and they are in parallel to the 279.0-keV transition. The 148.8-keV transition occurs in series of those transitions. The above consideration gives the energy difference of 428 keV between the initial and the final state of those cascade transitions. It is 26 keV smaller than the excitation energy of the isomeric state, 454(10) keV, measured by the ESR at GSI Darmstadt [9]. It may suggest that the γ rays measured in this work follow the transition with 26-keV energy difference from the previously reported isomeric state $^{195\mathrm{m}}$Os. Figure 4 shows one of possible decay schemes.

The half-life of the neutral isomer $^{195\mathrm{m}}$Os obtained in this work, 47(3) s, is much shorter than one of the full-strip isomer $^{195\mathrm{m}}\mathrm{Os}^{76+}$ measured at GSI, >9 min. It would be owing to the contribution of the internal conversion on the neutral $^{195\mathrm{m}}$Os atom. Because the binding energies of the K-shell and L-shell electrons of the osmium are 73.869 keV and 10.868 keV, respectively, the 26-keV transition from the isomeric state is dominated by the internal conversion of electrons in higher shells than K shell. The lifetime of the isomeric state strongly depends on its ionic charge. Table I lists the ranges of conversion coefficients, α, evaluated by BrIcc [18] for the 26-keV transition with possible multipolarities including the uncertainty of 10 keV. The ranges of the partial half-lives of γ transition, $T^{\gamma}_{1/2}$, calculated from the total half-life of 47 s and conversion coefficients are also listed in Table I. Considering the limitation of the half-life of $^{195\mathrm{m}}\mathrm{Os}^{76+}$, all multipolarities are possible.

The Weisskopf estimation for half-lives of electric and magnetic transitions, $T^{\mathrm{W}}_{1/2}$, [19] and the enhancement factor of γ transition probability to the Weisskopf estimation defined as $T^{\mathrm{W}}_{1/2}/T^{\gamma}_{1/2}$ are listed in Table I. Figure 5 shows decay schemes of $13/2^{+}$ isomeric states for isotones of ^{195}Os, ^{197}Pt [20] and ^{199}Hg [21]. Both reveal the cascade transitions from $13/2^{+}$ isomeric states to the $1/2^{-}$ ground states via $5/2^{-}$ excited states. The transitions from isomers are $M4$ and $M4+E5$ for ^{197}Pt and ^{199}Hg, respectively. Because the conversion coefficient for the transition of $^{197\mathrm{m}}$Pt is 7.71 [20], its γ transition partial half-life is 13.9 y. The Weisskopf estimation

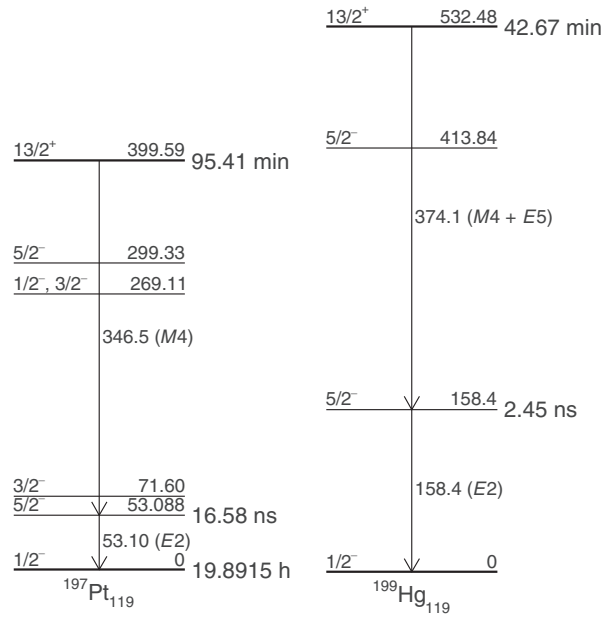

FIG. 5. Decay schemes of $13/2^{+}$ isomeric states for ^{197}Pt [20] and ^{199}Hg [21].

of its half-life is 21.1 h and the enhancement factor becomes $T^{W}_{1/2}/T^{\gamma}_{1/2} = 1.7 \times 10^{-4}$. If we assume the enhancement factor of similar order of magnitude for the transition from ^{195m}Os, $M2$ and $E3$ transitions are most probable.

The spectrum in Fig. 1 is in coincidence with the MSPGC hit pattern "$M = 1$". It means that the MSPGC was triggered with x rays or low-energy electrons less than around 200 keV. Four peaks on the spectrum corresponding to γ transitions of interest following the isomeric decay have different origins of their coincident events of the MSPGC; conversion electrons from other cascaded transitions and x rays following the internal conversion. However, if we assume that those four transitions are $M1$ or $E2$ transitions, their conversion coefficients are at least three orders of magnitude smaller than the conversion coefficient of the 26-keV $M2$ and $E3$ transition. Because the detection efficiency of the MSPGC for x rays is a few percents including fluorescence probabilities [16], the dominant trigger on the MSPGC in coincidence with the four γ transitions in the spectrum is considered to be x rays following the internal conversion of the 26-keV transition. Thus the relative γ-ray intensities of those four transitions are evaluated from their detected coincident counts and the detection efficiency of the HPGe clover detectors as indicated by italic figures in Fig. 4. Here detected coincident counts were evaluated from the growth-decay fitting of the time distributions in Fig. 2 using the constant half-life of 47 s.

The isomeric state of ^{195}Os is expected to have the spin-parity of $13/2^+$ in the systematics of its isotones. Because the ground state of ^{193}Os has the spin-parity of $3/2^-$ [22], the ground state of ^{195}Os is also expected to have the spin-parity of $3/2^-$ [17]. It is different from the spin-parity of $1/2^-$ for the ground states of its isotones, ^{197}Pt and ^{199}Hg. It may cause the difference of decay schemes of ^{195}Os from its isotones. Further spectroscopic studies of osmium isotopes and their isotones are desired for comprehensive understanding of structural evolution in W, Os, and Pt region.

In summary, we have measured γ rays associated with an isomeric decay of the ^{195}Os, and found four transitions with energies 111.0(1), 148.8(2), 168.8(2), and 279.0(2) keV for the first time. The half-lives characteristic to those four transitions agree with each other within their errors, indicating that they follow one isomeric decay with a half-life of 47(3) s. Correlation analysis of γ-γ coincidence and comparison with previous measurement obtained with the ESR at GSI Darmstadt suggests a possible decay scheme of ^{195m}Os, where cascade transitions observed in this work follows an isomeric decay with the energy of 26(10) keV. The discrepancy of half-lives of the isomeric state, 47(3) s for the neutral atom ^{195m}Os in this work and >9 min for the full-strip ion ^{195m}Os^{76+} at GSI, would be caused by the dominance of the internal conversion at such low-energy transition.

This experiment was performed at RI Beam Factory operated by RIKEN Nishina Center and CNS, University of Tokyo. The authors gratefully acknowledge the accelerator staff for their support. This work was supported by JSPS KAKENHI Grants No. 23244060, 24740180, 26247044, 15H02096, 17H01132, and 18H03711.

[1] K. Nomura, T. Otsuka, R. Rodríguez-Guzmán, L. M. Robledo, P. Sarriguren, P. H. Regan, P. D. Stevenson, and Zs. Podolyák, Spectroscopic calculations of the low-lying structure in exotic Os and W isotopes, Phys. Rev. C **83**, 054303 (2011).

[2] L. Robledo, R. Rodríguez-Guzmán, and P. Sarriguren, Role of triaxiality in the ground-state shape of neutron-rich Yb, Hf, W, Os and Pt isotopes, J. Phys. G **36**, 115104 (2009).

[3] P. Sarriguren, R. Rodríguez-Guzmán, and L. M. Robledo, Shape transitions in neutron-rich Yb, Hf, W, Os, and Pt isotopes within a Skyrme Hartree-Fock + BCS approach, Phys. Rev. C **77**, 064322 (2008).

[4] P. D. Stevenson, M. P. Brine, Z. Podolyak, P. H. Regan, P. M. Walker, and J. Rikovska Stone, Shape evolution in the neutron-rich tungsten region, Phys. Rev. C **72**, 047303 (2005).

[5] P. Möller, J. R. Nix, W. D. Myers, and W. J. Swiatecki, Nuclear ground-state masses and deformations, At. Data Nucl. Data Tables **59**, 185 (1995).

[6] C. Wheldon, J. Garcés Narro, C. J. Pearson, P. H. Regan, Z. Podolyák, D. D. Warner, P. Fallon, A. O. Macchiavelli, and M. Cromaz, Yrast states in ^{194}Os: The prolate-oblate transition region, Phys. Rev. C **63**, 011304(R) (2000).

[7] N. Al-Dahan, P. H. Regan, Zs. Podolyák, P. M. Walker, N. Alkhomashi, G. D. Dracoulis, G. Farrelly, J. Benlliure, S. B. Pietri, R. F. Casten *et al.*, Multiple β^- decaying states in ^{194}Re: Shape evolution in neutron-rich osmium isotopes, Phys. Rev. C **85**, 034301 (2012).

[8] S. Steer, Zs. Podolyák, S. Pietri, M. Górska, H. Grawe, K. H. Maier, P. H. Regan, D. Rudolph, A. B. Garnsworthy, R. Hoischen *et al.*, Isomeric states observed in heavy neutron-rich nuclei populated in the fragmentation of a ^{208}Pb beam, Phys. Rev. C **84**, 044313 (2011).

[9] M. Reed, P. M. Walker, I. J. Cullen, Yu. A. Litvinov, D. Shubina, G. D. Dracoulis, K. Blaum, F. Bosch, C. Brandau, J. J. Carroll *et al.*, Long-lived isomers in neutron-rich $Z = 72$ 76 nuclides, Phys. Rev. C **86**, 054321 (2012).

[10] Y. X. Watanabe, Y. H. Kim, S. C. Jeong, Y. Hirayama, N. Imai, H. Ishiyama, H. S. Jung, H. Miyatake, S. Choi, J. S. Song *et al.*, Pathway for the Production of Neutron-Rich Isotopes Around the $N = 126$ Shell Closure, Phys. Rev. Lett. **115**, 172503 (2015).

[11] J. Valiente-Dobon, P. H. Regan, C. Wheldon, C. Y. Wu, N. Yoshinaga, K. Higashiyama, J. F. Smith, D. Cline, R. S. Chakrawarthy, R. Chapman *et al.*, ^{136}Ba studied via deep-inelastic collisions: Identification of the $(\nu h_{11/2})^{-2}_{10+}$ isomer, Phys. Rev. C **69**, 024316 (2004).

[12] P. H. Regan, J. J. Valiente-Dobón, C. Wheldon, C. Y. Wu, J. F. Smith, A. O. Macchiavelli, D. Cline, R. S. Chakrawarthy, R. Chapman, M. Cromaz *et al.*, Production of exotic nuclear isomers in multi-nucleon transfer reactions, Laser Phys. Lett. **1**, 317 (2004).

[13] Y. Hirayama, Y. X. Watanabe, N. Imai, H. Ishiyama, S. C. Jeong, H. Miyatake, M. Oyaizu, S. Kimura, M. Mukai, Y. H. Kim *et al.*, Laser ion source for multi-nucleon transfer reaction products, Nucl. Instrum. Methods Phys. Res. B **353**, 4 (2015).

[14] Y. Hirayama, Y. X. Watanabe, M. Mukai, M. Oyaizu, M. Ahmed, H. Ishiyama, S. C. Jeong, Y. Kakiguchi, S. Kimura,

J. Y. Moon *et al.*, Doughnut-shaped gas cell for KEK isotope separation system, Nucl. Instrum. Methods Phys. Res. B **412**, 11 (2017).

[15] Y. Hirayama, M. Mukai, Y. Watanabe, M. Oyaizu, M. Ahmed, Y. Kakiguchi, S. Kimura, H. Miyatake, P. Schury, M. Wada, and S.-C. Jeong, Ionization cross section, pressure shift and isotope shift measurements of osmium, J. Phys. B **50**, 215203 (2017).

[16] M. Mukai, Y. Hirayama, Y. X. Watanabe, P. Schury, H. S. Jung, M. Ahmed, H. Haba, H. Ishiyama, S.C. Jeong, Y. Kakiguchi *et al.*, High-efficiency and low-background multi-segmented proportional gas counter for β-decay spectroscopy, Nucl. Instrum. Methods Phys. Res. A **884**, 1 (2018).

[17] X. Huang and M. Kang, Nuclear data sheets for $A = 195$, Nucl. Data Sheets **121**, 395 (2014).

[18] T. Kibédi, T. W. Burrows, M. B. Trzhaskovskaya, P. M. Davidson, and C. W. Nestor Jr., Evaluation of theoretical conversion coefficients using BrIcc, Nucl. Instrum. Methods Phys. Res. A **589**, 202 (2008).

[19] R. B. Firestone, APPENDIX K, in *Table of Isotopes*, 8th ed., edited by C. M. Beglin and S. Y. F. Chu (Wiley-VCH, Weinheim, 1999).

[20] X. Huang and C. Zhou, Nuclear data sheets for $A = 197$, Nucl. Data Sheets **104**, 283 (2005).

[21] B. Singh, Nuclear data sheets for $A = 199$, Nucl. Data Sheets **108**, 79 (2007).

[22] M. S. Basunia, Nuclear data sheets for $A = 193$, Nucl. Data Sheets **143**, 1 (2017).